THIRD EDITION

Fundamentals of Creep in Metals and Alloys

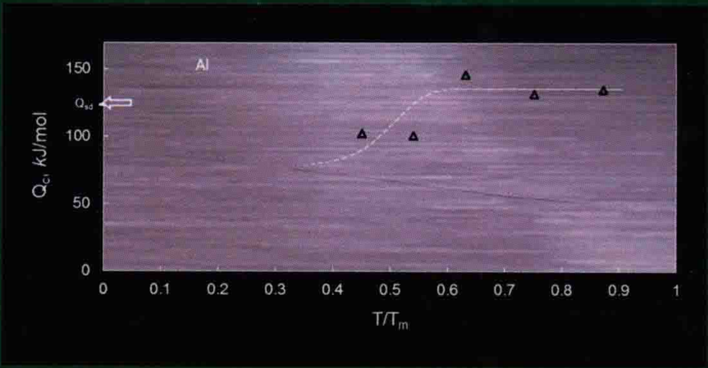

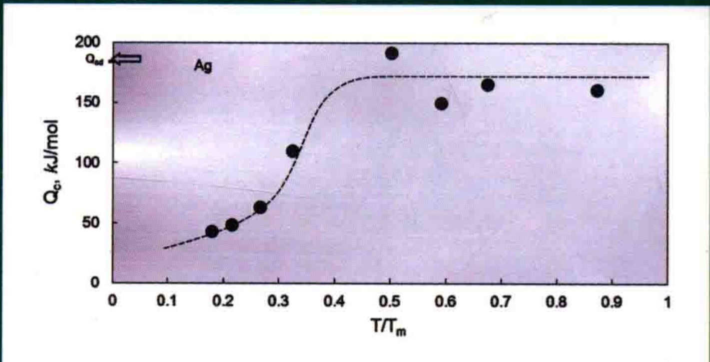

The variation of the activation energy for creep versus fraction of the melting temperature for Al (top) and Ag (bottom)

M. E. KASSNER

Fundamentals of
CREEP IN METALS AND ALLOYS

THIRD EDITION

M.E. KASSNER
Departments of Aerospace and Mechanical Engineering,
Chemical Engineering, and Materials Science
University of Southern California
Los Angeles, CA
USA

ELSEVIER

AMSTERDAM • BOSTON • HEIDELBERG • LONDON
NEW YORK • OXFORD • PARIS • SAN DIEGO
SAN FRANCISCO • SINGAPORE • SYDNEY • TOKYO
Butterworth-Heinemann is an imprint of Elsevier

B H

Butterworth Heinemann is an imprint of Elsevier
225 Wyman Street, Waltham, MA 02451, USA
The Boulevard, Langford Lane, Kidlington, Oxford, OX5 1GB, UK

ISBN: 978-0-08-099427-7

British Library Cataloguing in Publication Data
A catalogue record for this book is available from the British Library

Library of Congress Cataloging-in-Publication Data
A catalog record for this book is available from the Library of Congress

For information on all Butterworth Heinemann publications visit our web site at http://store.elsevier.com

Printed in the United States of America

PREFACE

This book on the fundamentals of creep plasticity is a review and analysis of investigations in a variety of areas relevant to creep plasticity. These areas include five-power-law creep, which is sometimes referred to as dislocation climb-controlled creep (in metals, alloys, and ceramics), viscous glide or three-power-law creep (in alloys), diffusional creep, Harper–Dorn creep, superplasticity, second-phase strengthening, and creep cavitation and fracture. Many quality reviews and books precede this attempt to write an extensive review of creep fundamentals and the improvement was a challenge. One advantage with this attempt is the ability to describe the substantial work published subsequent to these earlier reviews. An attempt was made to cover the basic work discussed in these earlier reviews but especially to emphasize more recent developments.

This is the second edition of this book and one aspect of this recent edition is correcting errors in the first edition, also, many advances occurred over the five years since the first edition and theses are also incorporated. Dr Maria-Teresa Perez-Prado was a co-author of the first edition. While she did not participate in the formulation of the second and third editions, Chapters 5, 6, and 9 remain largely a contribution by Dr Perez-Prado, and her co-authorship is indicated on these chapters.

LIST OF SYMBOLS AND ABBREVIATIONS

a	Cavity radius
a_0	Lattice parameter
$A' - A''''$	Constants
A, A_F, A_{C-J}, A_{APB}, A_{SN}, A_{CR}	Solute dislocation interaction parameters
A_{gb}	Grain boundary area
A_{HD}	Harper–Dorn equation constant
A_{PL}	Constants
A_v	Projected area of void
A_0–A_{12}	Constant
APB	Antiphase boundary
b	Burgers vector
B	Constant
BMG	Bulk metallic glass
c	Concentration of vacancies
c^*	Crack growth rate
c_j	Concentration of jogs
c_p	Concentration of vacancies in the vicinity of a jog
c_p^*	Steady-state vacancy concentration near a jog
c_v	Equilibrium vacancy concentration
c_v^D	Vacancy concentration near a node or dislocation
c_0	Initial crack length
c_{1-2}	Constants
C	Concentration of solute atoms
C^*	Integral for fracture mechanics of time-dependent plastic materials
C_{1-2}	Constant
C_{LM}	Larson–Miller constant
CBED	Convergent beam electron diffraction
CGBS	Cooperative grain boundary sliding
CS	Crystallographic slip
CSF	Complex stacking fault
CSL	Coincident site lattice
C_0^*	Constant
C_0–C_5	Constants
d	Average spacing of dislocations that comprise a subgrain boundary
D	General diffusion coefficient or constant
D'	Constant

D_c	Diffusion coefficient for climb
D_{eff}	Effective diffusion coefficient
D_g	Diffusion coefficient for glide
D_{gb}	Diffusion coefficient along grain boundaries
D_i	Interfacial diffusion
D_s	Surface diffusion coefficient
D_{sd}	Lattice self-diffusion coefficient
D_v	Diffusion coefficient for vacancies
D_0	Diffusion constant
DRX	Discontinuous dynamic recrystallization
$\tilde{D}$	Diffusion coefficient for the solute atoms
e	Solute–solvent size difference or misfit parameter
E	Young's modulus or constant
E_j	Formation energy for a jog
EBSP	Electron backscatter patterns
f	Fraction
f_m	Fraction of mobile dislocations
f_p	Chemical dragging force on a jog
f_{sub}	Fraction of material occupied by subgrains
F	Total force per unit length on a dislocation
FEM	Finite element method
g	Average grain size (diameter)
g'	Constant
G	Shear modulus
GBS	Grain boundary sliding
GDX	Geometric dynamic recrystallization
GNB	Geometrically necessary boundaries
h_r	Hardening rate
$\bar{h}_m$	Average separation between slip planes within a subgrain with gliding dislocations
h	Dipole height or strain-hardening coefficient
HAB	High angle boundary
HVEM	High voltage transmission electron microscopy
j	Jog spacing
J	Integral for fracture mechanics of plastic material
J_{gb}	Vacancy flux along a grain boundary
k	Boltzmann constant
k'–k'''	Constants
k_y	Hall–Petch constant
k_{MG}	Monkman–Grant constant
k_R	Relaxation factor
k_1–k_{10}	Constants
K	Strength parameter or constant
K_I	Stress intensity factor
K_0–K_7	Constants
ℓ	Link length of a Frank dislocation network
ℓ_c	Critical link length to unstably bow a pinned dislocation

ℓ_m	Maximum link length
l	Migration distance for a dislocation in Harper–Dorn creep
L	Particle separation distance
LAB	Low angle boundary
LM	Larson–Miller parameter
LRIS	Long-range internal stress
m	Strain-rate sensitivity exponent ($=1/N$)
m'	Transient creep time exponent
m''	Strain-rate exponent in the Monkman–Grant equation
m_c	Constant
$\overline{M}$	Average Taylor factor for a polycrystal
M_ρ	Dislocation multiplication constant
n	Steady-state creep exponent or strain-hardening exponent
n^*	Equilibrium concentration of critical sized nuclei
n_m	Steady-state stress exponent of the matrix in a multi-phase material
N	Constant structure stress exponent and dislocation link length per unit volume
$\dot{N}$	Nucleation rate and rate of release of dislocation loops
p	Steady-state dislocation density stress exponent
p'	Inverse grain size stress exponent for superplasticity
PLB	Power law breakdown
POM	Polarized light optical microscopy
PSB	Persistent slip band
q	Dislocation spacing, d, stress exponent
Q_c	Activation energy for creep (with E or G compensation)
Q'_c	Apparent activation energy for creep (no E or G compensation)
Q_p	Activation energy for dislocation pipe diffusion
Q_{sd}	Activation energy for lattice self-diffusion
Q_v	Formation energy for a vacancy
Q^*	Effective activation energies in composites where load transfer occurs
r_r	Recovery rate
R_o	Diffusion distance
R_s	Radius of solvent atoms
s	Structure
SAED	Selected area electron diffraction
SESF	Superlattice extrinsic stacking fault
SISF	Superlattice intrinsic stacking fault
STZ	Shear transformation zone
t	Time
t_c	Time for cavity coalescence on a grain boundary facet
t_f	Time to fracture (rupture)
t_s	Time to the onset of steady-state
T	Temperature
T_d	Dislocation line tension
T_g	Glass transition temperature
T_m	Melting temperature
T_p	Temperature of the peak yield strength

T_x	Onset crystallization temperature
TEM	Transmission electron microscopy
$T-T-T$	Time–temperature–transformation diagram
v	Dislocation glide velocity
v_c	Dislocation climb velocity
v_{cr}	Critical dislocation velocity at breakaway
v_D	Debye frequency
v_p	Jog climb velocity
$\bar{v}$	Average dislocation velocity
$\bar{v}_\ell$	Climb velocity of dislocation links of a Frank network
V	Activation volume
w	Width of a grain boundary
$\bar{x}_c$	Average dislocation climb distance
$\bar{x}_g$	Average dislocation slip length due to glide
XRD	X-ray diffraction
α	Taylor equation constant
α_o	Constant
α'	Climb resistance parameter
α_{1-3}	Constants
β, β_{1-3}	Constants
γ	Shear strain
γ_o	Characteristic strain of an STZ
γ_A	Anelastic unbowing strain
γ_{gb}	Interfacial energy of a grain boundary
γ_m	Surface energy of a metal
$\dot{\gamma}$	Shear creep rate
$\dot{\gamma}_{ss}$	Steady-state shear creep rate
δ	Grain boundary thickness or lattice misfit
Δa	Activation area
ΔG	Gibbs free energy
ΔV_C	Activation volume for creep
ΔV_L	Activation volume for lattice self-diffusion
ϵ	Uniaxial strain
ϵ_o	Instantaneous strain
$\dot{\epsilon}$	Strain rate
$\dot{\epsilon}_{min}$	Minimum creep rate
$\dot{\epsilon}_{ss}$	Steady-state uniaxial strain rate
$\bar{\epsilon}$	Effective uniaxial or von Mises strain
θ	Misorientation angle across high-angle grain boundaries
θ_λ	Misorientation angle across (low-angle) subgrain boundaries
$\theta_{\lambda ave}$	Average misorientation angle across (low-angle) subgrain boundaries
λ	Average subgrain size (usually measured as an average intercept)
λ_s	Cavity spacing
λ_{ss}	Average steady state subgrain size
ν	Poisson's ratio
ν_o	Attempt frequency (often Debye frequency)
ρ	Density of dislocations not associated with subgrain boundaries

ρ_m	Mobile dislocation density
ρ_{ms}	Mobile screw dislocation density
ρ_{ss}	Steady-state dislocation density not associated with subgrain walls
σ	Applied uniaxial stress
σ_i	Internal stress
σ_o	Single crystal yield strength
σ'_o	Annealed polycrystal yield strength
σ''_o	Sintering stress for a cavity
σ_p	Peierls stress
σ_{ss}	Uniaxial steady-state stress
σ_T	transition stress between five-power law and Harper–Dorn creep
σ_{TH_s}	Threshold stress for superplastic deformation
$\sigma_y\big\vert_{T,\dot{\epsilon}}$	Yield or flow stress at a reference temperature and strain rate
$\sigma_y^{0.002}$	0.2% offset yield stress
$\overline{\sigma}$	Effective uniaxial, or von Mises, stress
τ	Shear stress
τ_b	Breakaway stress of the dislocations from solute atmospheres
τ_c	Critical stress for climb over a second phase particle
τ_d	Detachment stress from a second phase particle
τ_j	Stress to move screw dislocations with jogs
τ_{or}	Orowan bowing stress
τ_B	Shear stress necessary to eject dislocation from a subgrain boundary
τ_{BD}	Maximum stress from a simple tilt boundary
τ_L	Stress to move a dislocation through a boundary resulting from jog creation
τ_N	Shear strength of a Frank Network
$(\tau/G)_t$	Normalized transition stress
$\phi(P)$	Frank network frequency distribution function
χ	Stacking fault energy
χ'	Primary creep constant
ψ	Angle between cavity surface and projected grain boundary surface
ω_m	Maximum interaction energy between a solute atom and an edge dislocation
Ω	Atomic volume
ω	Fraction of grain boundary area cavitated

CONTENTS

CHAPTER 1

Fundamentals of Creep in Materials

Contents

1. INTRODUCTION

1.1 Description of Creep

Creep of materials is classically associated with time-dependent plasticity under a fixed stress at an elevated temperature, often greater than roughly 0.5 T_m, where T_m is the absolute melting temperature. The plasticity under these conditions is described in Figure 1 for constant stress (a) and constant strain rate (b) conditions. Several aspects of the curve in Figure 1 require explanation. First, three regions are delineated: Stage I, or primary creep, which denotes that portion where (in (a)) the creep rate (plastic strain rate), $\dot{\varepsilon} = d\varepsilon/dt$ is changing with increasing plastic strain or time. In Figure 1(a), the primary creep rate decreases with increasing strain, but with some types of creep, such as solute drag with "3-power creep," an "inverted" primary occurs where the strain rate increases with strain. Analogously, in (b), under constant strain rate conditions, the metal hardens, resulting in increasing flow stresses. Often, in pure metals, the strain rate decreases or the stress increases to a value that is constant over a range of strain. The phenomenon is termed Stage II, secondary, or steady-state (SS) creep. Eventually, cavitation and/or cracking increases the apparent strain rate or decreases the flow stress. This regime is termed Stage III, or tertiary, creep and leads to fracture. Sometimes, Stage I leads directly to Stage III and an "inflection" is observed. Thus, care must sometimes be exercised in concluding a mechanical SS.

The term "creep" as applied to plasticity of materials likely arose from the observation that at modest and constant stress, at or even below the macroscopic yield stress of the metal (at a "conventional" strain rate), plastic deformation occurs over time as described in Figure 1(a). This is in contrast

Fundamentals of Creep in Metals and Alloys
ISBN 978-0-08-099427-7
http://dx.doi.org/10.1016/B978-0-08-099427-7.00001-3

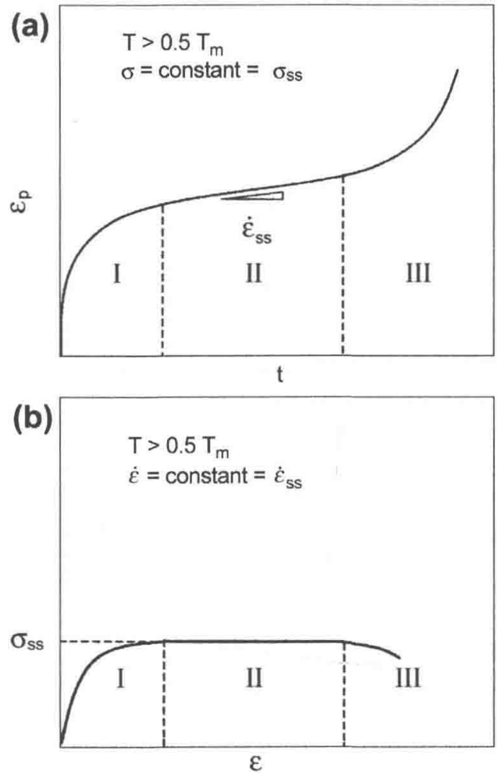

Figure 1 Constant true stress and constant strain rate creep behavior in pure and Class M (or Class I) metals.

with the *general* observation, such as at ambient temperature, where a material deformed at, for example, 0.1–0.3 T_m, shows very little plasticity under constant stress at or below the yield stress, again, at "conventional" or typical tensile testing strain rates (e.g., 10^{-4}–10^{-3} s^{-1}). (The latter observation is not always true as it has been observed that some primary creep is observed (e.g., a few percent strain, or so) over relatively short periods of time at stresses less than the yield stress (e.g., [1,2])).

We observe in Figure 2 that at the "typical" testing strain rate of about 10^{-4} s^{-1}, the yield stress is σ_{y1}. However, if we decrease the testing strain rate to, for example, 10^{-7} s^{-1}, the yield stress decreases significantly, as will be shown is common for metals and alloys at high temperatures. To a "first approximation," we might consider the microstructure (created by dislocation microstructure evolution with plasticity) at just 0.002 plastic strain to be independent of $\dot{\varepsilon}$. In this case, we might describe the change in yield

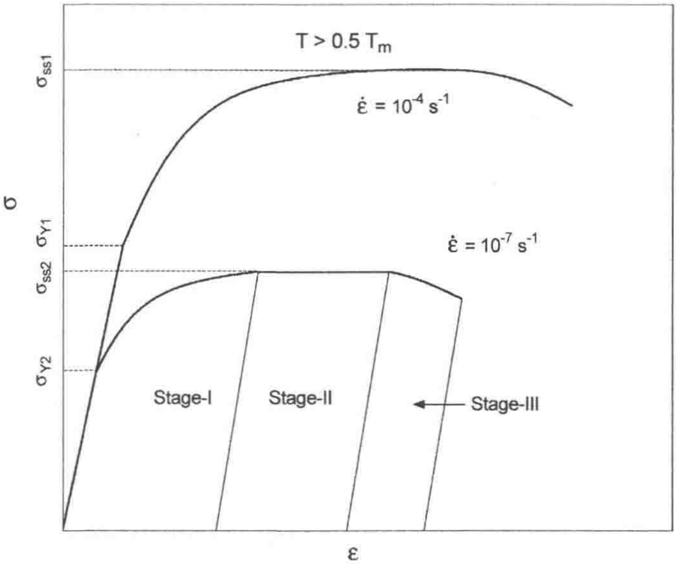

Figure 2 Creep behavior at two different constant strain rates.

stress to be the sole result of the $\dot{\varepsilon}$ change and predicted by the "constant structure" stress-sensitivity exponent, N, defined by.

$$N = [\partial \ln \dot{\varepsilon} / \partial \ln \sigma]_{T,s} \tag{1}$$

where T and s refer to temperature and the substructural features, respectively. Sometimes, the sensitivity of the creep rate to changes in stress is described by a constant structure strain-rate sensitivity exponent, $m = 1/N$. Generally, N is relatively high at lower temperatures [3] which implies that significant changes in the strain rate do not dramatically affect the flow stress. In pure fcc metals, N is typically between 50 and 250 [3]. At higher temperatures, the values may approach 10, or so [3–10]. N is graphically described in Figure 3. The trends of N versus temperature for nickel are illustrated in Figure 4.

Another feature of the hypothetical behaviors in Figure 2 is that (at the identical temperature) not only is the yield stress at a strain rate of 10^{-7} s^{-1} lower than it is at 10^{-4} s^{-1}, but also the peak stress or, perhaps, SS stress, which is maintained over a substantial strain range, is *less* than the yield stress at a strain rate of 10^{-4} s^{-1}. (Whether SS occurs at, for example, ambient temperature has not been fully settled, as large strains are not easily achievable. Stage IV and/or recrystallization may preclude this SS [11–13].)